

# Uplink NOMA for UAV-Aided Maritime Internet-of-Things

Nikolaos Nomikos<sup>1</sup>, Anastasios Giannopoulos<sup>1</sup>, Panagiotis Trakadas<sup>1</sup>, and George K. Karagiannidis<sup>2,3</sup>

<sup>1</sup>Department of Ports Management and Shipping,  
National and Kapodistrian University of Athens, Greece

<sup>2</sup>Aristotle University of Thessaloniki, Greece

<sup>3</sup>Cyber Security Systems and Applied AI Research Center, Lebanese American University (LAU), Lebanon  
nomikosn@pms.uoa.gr, angianno@uoa.gr, akalafat@core.uoa.gr, ptrakadas@uoa.gr, geokarag@auth.gr

**Abstract**—Maritime activities are vital for economic growth, being further accelerated by various emerging maritime Internet-of-Things (IoT) use cases, including smart ports, autonomous navigation, and ocean monitoring systems. However, broadband, low-delay, and reliable wireless connectivity to the ever-increasing number of vessels, buoys, platforms and sensors in maritime communication networks (MCNs) has not yet been achieved. Towards this end, the integration of unmanned aerial vehicles (UAVs) in MCNs provides an aerial dimension to current deployments, relying on shore-based base stations (BSs) with limited coverage and satellite links with high latency. In this work, a maritime IoT topology is examined where direct uplink communication with a shore BS cannot be established due to excessive path-loss. In this context, we employ multiple UAVs for end-to-end connectivity, simultaneously receiving data from the maritime IoT nodes, following the non-orthogonal multiple access (NOMA) paradigm. In contrast to other UAV-aided NOMA schemes in maritime settings, dynamic decoding ordering at the UAVs is used to improve the performance of successive interference cancellation (SIC), considering the rate requirements and the channel state information (CSI) of each maritime node towards the UAVs. Moreover, the UAVs are equipped with buffers to store data and provide increased degrees of freedom in opportunistic UAV selection. Simulations reveal that the proposed opportunistic UAV-aided NOMA improves the average sum-rate of NOMA-based maritime IoT communication, leveraging the dynamic decoding ordering and caching capabilities of the UAVs.

**Index Terms**—Maritime Communication Networks, Maritime Internet-of-Things, Non-Orthogonal Multiple Access (NOMA), Opportunistic Selection, Unmanned Aerial Vehicle (UAV).

## I. INTRODUCTION

In recent years, the fifth generation (5G) of mobile communications has focused on the coexistence of mobile users and Internet-of-Things (IoT) devices, being mainly located in urban environments [1]–[3]. As a result, the majority of network architectures and communication techniques were designed for land-based communications, while maritime communication networks (MCNs) have not exploited the tremendous advances in wireless communications. Usually, MCNs are supported from satellites, characterized by well-known issues, such as high-latency and low-data rates [4]. Considering that the vast majority of trade relies on maritime transportation, while the interest for a wide range of maritime activities, including ocean monitoring, as well as improved security and safety, has spiked, a radical shift to maritime communications is needed

[5]. In this context, the integration of unmanned aerial vehicles (UAVs) in wireless networks represents a unique opportunity for ubiquitous coverage at sea [6]–[8]. UAVs flexibly provide radio-resources adhering to the Quality-of-Service (QoS) requirements of applications while being capable of operating autonomously, offering high reliability and low-latency.

Thus, it is important to study the potential of UAVs to serve maritime IoT applications, leveraging novel communications techniques. In this paper, a maritime IoT topology is examined where a UAV is deployed to establish end-to-end uplink connectivity with a shore base station (BS). The maritime IoT nodes transmit simultaneously under the non-orthogonal multiple access (NOMA) paradigm, and the UAV successively decodes their data prior to forwarding them to the BS [9]–[11].

### A. Maritime communication networks

MCNs support a plethora of applications, including smart navigation, offshore facility operation, ocean exploration, pollution monitoring, and search and rescue (SAR) operations [12]. The maritime IoT ecosystem comprises a heterogeneous mix of vessels, buoys, platforms, unmanned surface vehicles (USVs) and unmanned underwater vehicles (UUVs), sensors, and actuators [6]. Also, maritime services have diverse QoS requirements, since, for example, crew and passengers on-board cruise ships might be interested in broadband connectivity, security operations entail the transmission of underwater video or images, while IoT services in smart maritime environments and intelligent transportation systems are based on ultra-reliable and ultra-low latency (URLLC) [13].

Currently, wireless coverage for MCNs relies on shore-based base stations (BSs) and satellite constellations. However, these options have inherent drawbacks, i.e. low data rates and high communication delays, especially for the satellite segment, insufficient spectrum, and unreliable connectivity. Recent industrial initiatives have targeted broadband satellite coverage and long-distance shore-to-vessel communications using cellular standards [14], [15]. Still, the aerial dimension where UAVs can mitigate the impact of geographical characteristics on path-loss, reduce communication delays, enhance communication reliability and offer dynamic resource provisioning has not been adequately explored in maritime IoT topologies.

## B. UAV-aided wireless networks

6G networks depart from conventional architectures, integrating moving nodes for dynamic resource provisioning and increased network resiliency [16]. In this domain, UAVs efficiently complement terrestrial and satellite networks, offering coverage in remote and rural settings, quick recovery after disasters, and on-demand provisioning of radio-resources [6], [17]. In maritime settings, the use of UAVs to ensure broadband connectivity or URLLC for offshore facilities, search and rescue operations and IoT applications has attracted significant interest in recent years [18], [19]. More specifically, UAVs can assume the role of wireless relays, enabling multi-hop communication between shore BSs and maritime nodes. In the underwater IoT, UAVs can facilitate data collection by cooperating with USVs and UUVs [20].

NOMA-based and UAV-aided MCNs have been studied in a small number of works. Fang *et al.* in [21], establish a collaborative nearshore network relying on shore BSs and UAVs and forming user-centric virtual clusters. A joint power allocation problem is presented for sum-rate maximization with interference mitigation among different network segments, clusters, and users. Since the problem is shown to be non-convex with intractable non-linear constraints, an iterative power allocation algorithm is proposed, offering improved coverage, compared to other orthogonal multiple access (OMA) and NOMA schemes. Furthermore, Tang *et al.* in [11] study NOMA groups, comprising vessels that are served either by UAVs or shore BSs. In order to reduce the overall system cost, a single-antenna UAV has been considered with a trajectory dictated by vessels located in blind zones. Performance evaluation shows improved spectral efficiency, compared to OMA. In terms of energy efficiency, Ma *et al.* in [22], [23] proposed an architectural approach where UAV relays collect data from surface sink nodes (SNs), controlling underwater sensor nodes (USNs) and forward them to a shore BS. Towards maximizing the network's lifetime, resource allocation and UAV deployment are modelled as a non-convex optimization problem and decoupled into a delay minimization subproblem for the UAV-SN communication and lifetime maximization subproblem for the USN-SN communication. Simulations verify that improved performance is achieved over OMA-based approaches.

## C. Contributions

In this paper, a maritime IoT topology is studied where direct communication towards a shore BS is not possible due to path-loss. Thus, we employ multiple UAVs, acting as relays, concurrently receiving data from the maritime IoT nodes. Contrary to the scheme of [22], [23], we adopt dynamic decoding ordering at the UAVs to improve the performance of successive interference cancellation (SIC), considering both data rate requirements and the CSI of each maritime node towards the UAVs. Also, the UAVs are equipped with buffers, facilitating opportunistic UAV selection for reception/transmission of data. Simulation results show that the proposed UAV-aided NOMA enhances the communication reliability by exploiting the dynamic decoding ordering and the UAV buffers.

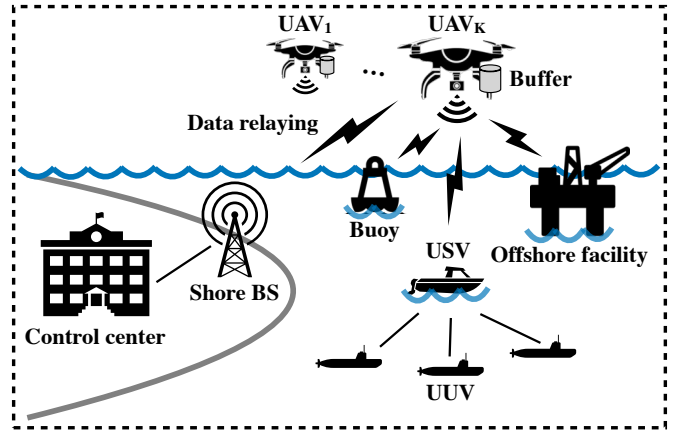


Fig. 1. A UAV-aided maritime IoT topology.

## II. SYSTEM MODEL

### A. Network model

A UAV-assisted MCN is considered, consisting of  $N$  maritime sources, e.g. USVs, buoys and offshore facilities,  $S_n$  ( $1 \leq n \leq N$ ), one destination (shore BS),  $D$ , and a cluster  $\mathcal{C}$  of  $K$  UAVs, acting as half-duplex (HD) decode-and-forward (DF) relays,  $R_k \in \mathcal{C}$  ( $1 \leq k \leq K$ ), as depicted in Fig. 1. Due to severe fading, the direct links between the transmitting maritime nodes and the shore BS do not exist and it is assumed that communication can only be established via the UAVs. Each UAV is equipped with a buffer of size  $L$ , denoting the maximum number of data elements that can be stored from the sources' transmissions. The number of packets in the buffer of the UAV  $R_k$  is denoted by  $Q_k$ . The buffer is allocated equally to each source i.e., the same amount of data elements of  $S_1, S_2, \dots, S_N$  can be stored at each UAV. This assumption results in the formation of sub-buffers, denoted as  $Q_{k,S_n}$  and the respective sub-buffer sizes, assumed to be equal at each relay are denoted by  $L_{S_n}$ .

The source nodes are assumed to be saturated (i.e., they always have data to transmit) and the required information rate,  $r_{S_n}$ , for successful reception at each UAV is fixed and may differ, depending on the application; for example, if  $S_1$  is a USV, controlling a number of underwater patrolling UUVs and  $S_2$  is a buoy, performing sea monitoring, the rate requirements differ and, hence,  $r_{S_1} \neq r_{S_2}$ . Likewise, a transmission from a transmitter  $i$  to its corresponding receiver  $j$  is successful if the signal-to-noise ratio (SNR)  $\Gamma_{ij}$  at the receiver is greater than or equal to a threshold  $\gamma_{ij}$ , called the *capture ratio*. More specifically,  $\gamma_{ij}$  is defined as  $\gamma_{ij} = 2^{r_i - 1}$ , where the value of  $r_i$  depends on the modulation and coding characteristics of the maritime IoT application. At each time-slot, the maritime nodes or one of the UAVs attempt to transmit a packet, attempt to transmit a packet, using a fixed power level  $P_i$ ,  $i \in \{S_1, \dots, S_N, R_1, \dots, R_K\}$ .

The retransmission process is based on an acknowledgement/negative-acknowledgement (ACK/NACK) mechanism, in which short-length error-free packets are broadcasted by

the receivers over a separate narrow-band channel. In addition, as more than one UAVs might receive the same packet, it is necessary to notify them on which packet(s) was received by the destination. Thus, the short-length ACK packets include the packet ID information, in order for the UAVs to drop the respective packet(s) from their queues and avoid duplicate transmissions at another time-slot.

### B. Channel model

Time is divided into “slots” of one packet duration. At any arbitrary time-slot  $t$ , the quality of the wireless channels is degraded by additive white Gaussian noise (AWGN), frequency non-selective small-scale block fading, according to a complex Gaussian distribution with zero mean and variance  $\sigma_{ij}^2$  for the  $\{i \rightarrow j\}$  link, and large-scale fading due to path-loss. The complex channel coefficient for the  $\{i \rightarrow j\}$  link is denoted by  $s_{ij}$ , and the channel gain,  $|s_{ij}|^2$ , is assumed to be exponentially non-identically distributed i.e.,  $|s_{ij}|^2 \sim \text{Exp}(\lambda_{ij})$ ,  $\lambda_{ij} > 0$ , as is the case of an asymmetric topology. The variance of thermal noise at a receiver  $l$  is denoted by  $\sigma_l^2$ ,  $l \in \{R_1, R_2, \dots, R_K, D\}$  and it is assumed to be distributed as AWGN, with zero mean and variance equal to  $\sigma_l^2$ .

The UAV-to-maritime node channel is dominated by the line-of-sight (LoS) and non-line-of-sight (NLoS) components, where the probability of LoS mainly depends on the density and height of scatterers in the coverage area and the elevation angle of the maritime node to UAV [24]. The large-scale fading coefficient between a maritime node  $i$  and a UAV  $j$  is given by [11], [25].

$$L_{ij}^{\text{dB}} = \frac{\eta_{LoS} - \eta_{NLoS}}{1 + \alpha e^{-b(\rho_{ij} - \alpha)}} + B_{ij}; \quad (1)$$

where

$$B_{ij} = 20 \log_{10}(d_{ij}) + 20 \log_{10}\left(\frac{4\pi f}{c}\right) + \eta_{NLoS}; \quad (2)$$

$$\rho_{ij} = \frac{180}{\pi} \arcsin\left(\frac{h_U}{d_{ij}}\right); \quad (3)$$

where  $f$  is the carrier frequency,  $c$  is the speed of light, and  $\eta_{LoS}$ ,  $\eta_{NLoS}$ ,  $\alpha$ ,  $b$  are constants related to the propagation environment, and  $h_U$  is the UAV altitude.

Therefore, the large-scale channel fading is expressed as

$$L_{ij} = 10^{-\frac{L_{ij}^{\text{dB}}}{10}}. \quad (4)$$

Thus, the channel coefficient, including both small- and large-scale fading is expressed as

$$h_{ij} = L_{ij}^{1/2} s_{ij}. \quad (5)$$

1) *Transmission in the  $\{S \rightarrow R\}$  link:* When transmission in the  $\{S \rightarrow R\}$  link occurs, the information symbols of the  $N$  sources, i.e.,  $x_1, \dots, x_N$  with  $\mathbb{E}[|x_n^2|] = 1$ ,  $n \in \{1, 2, \dots, N\}$  are transmitted concurrently, through NOMA.

Then, UAV  $R_k$  will receive signal  $y_k$ , containing the symbols of the  $N$  sources, given by

$$y_k = \sum_{n=1}^N h_{S_n R_k} \sqrt{P_{S_n}} x_n + N_{R_k}; \quad (6)$$

where  $N_{R_k}$  denotes the AWGN at the UAV  $R_k$ .

Regarding SIC operation, the signal of  $S_n$  can be successfully decoded at  $R_k$  if

$$\Gamma_{S_n R_k}(P_{S_n}) \triangleq \frac{|h_{S_n R_k}|^2 P_{S_n}}{\sum_{i=n+1}^N |h_{S_i R_k}|^2 P_{S_i} + \sigma_{R_k}^2} \geq 2^{r_{S_n}} - 1; \quad (7)$$

assuming that the previous  $N - n$  signals have been successfully decoded at  $R_k$ , being subtracted from  $y_k$  prior to decoding the signal of  $S_n$ .

For ordering the sources' signals, the dynamic SIC receiver of [26] is employed. This receiver relies on CSI at the UAVs to order the signals of the maritime nodes, based on the instantaneous received signal power. By denoting as  $\Phi$  the set of all possible decoding orders,  $R_k$  determines the permutation  $\phi_k$ ,  $\phi_k \in \Phi$  with which, the sources' signals are ordered. After an arbitrary broadcasting phase, each UAV sequentially decodes the signals by ordering the sources as  $\phi_{k,1}, \phi_{k,2}, \dots, \phi_{k,N}$ , according to their respective channel gains  $g_{\phi_{k,1} R_k} \geq g_{\phi_{k,2} R_k} \geq \dots \geq g_{\phi_{k,N} R_k}$ , as equal transmit power level is assumed at every source. So, the strongest signal is decoded first, by considering the other  $N - 1$  signals as interference. Then, SIC subtracts the decoded signal and moves on to the second strongest signal. This process is repeated until the weakest signal of the source with index  $\phi_{k,N}$  is decoded interference-free. The set of feasible  $\{S \rightarrow R\}$  links is denoted by  $\mathcal{F}_{SR}^n$ , having a cardinality of  $F_{SR}^n$ , where the UAV has successfully decoded packets of  $n$  sources after the dynamic SIC operation, and its members fulfill (7).

2) *Transmission in the  $\{R \rightarrow D\}$  link:* In practice, each maritime node might transmit at a different rate  $r_{S_n}$ , as diverse IoT applications are supported. Then, in order to avoid buffer overflow or starvation, the selected UAV  $R_k$  will forward a combined packet to the destination, transmitting at a maximum rate  $r_{\max} = \sum_{n=1}^N r_{S_n}$ , i.e., a rate equal to the sum of the rate requirements of the  $N$  maritime nodes. Therefore, if  $N$  packets are combined, the SNR at the destination should fulfill

$$\Gamma_{R_k D}(P_{R_k}) \triangleq \frac{|h_{R_k D}|^2 P_{R_k}}{\sigma_D^2} \geq 2^{r_{\max}} - 1. \quad (8)$$

On the contrary, the packet, containing the data of  $N$  sources will not be successfully transmitted to the shore BS, if  $\gamma_{R_k D} < 2^{r_{\max}} - 1$ . Thus, the outage probability for the simultaneous data transmission of  $N$  sources by  $R_k$  is expressed as follows

$$P_{\text{out}\{R \rightarrow D\}} \triangleq \Pr \left[ |h_{R_k D}|^2 < \frac{(2^{r_{\max}} - 1) \sigma_D^2}{P_{R_k}} \right]. \quad (9)$$

It should be noted that additional flexibility to the NOMA transmission is enabled, since when the proposed relaying algorithm is adopted, the number of packets being stored and transmitted is not strictly equal to  $N$ . More specifically, in terms of channel capacity, the worst case is equivalent to having a wireless channel supporting only the transmission of the maritime node requesting a service with the minimum rate requirement. In this case, the probability in (9) does not depend on  $r_{\max}$ , but on  $r_{\min}$ , where  $r_{\min} = \min\{r_1, r_2, \dots, r_N\}$  corresponds to the minimum rate requirement, in order to avoid a complete outage in the  $\{R \rightarrow D\}$  link.

Since in the considered topology, channel state information at the transmitter (CSIT) in the  $\{R \rightarrow D\}$  links is assumed to be available, the selected UAV employs rate adaptation, choosing a transmission rate, aiming to transmit packets from as many maritime sources as possible. By  $\mathcal{F}_{RD}^n$ , the set of feasible  $\{R \rightarrow D\}$  links is denoted, having a cardinality of  $F_{RD}^n$ , where the respective UAVs can transmit packets from  $n$  sources, residing in their buffers. On the contrary, if an  $\{R \rightarrow D\}$  link is feasible, i.e., it can support the transmission of a packet with rate  $r_{S_i}$ ,  $i \in \{1, 2, \dots, N\}$  but the relay's buffer is empty, that link is assumed to be in outage.

### III. UAV-AIDED NOMA FOR MARITIME IOT

Here, UAV selection in uplink MCNs, employing caching and dynamic decoding ordering at each UAV, establishing connectivity for  $N$  maritime IoT nodes (mIoT – NOMA) with a shore BS is discussed. The proposed algorithm is based on low complexity implementation, as maritime IoT nodes do need any CSI, thus being extremely useful in networks comprising resource-constrained devices and also, the required intelligence for SIC is transferred at the more capable UAVs.

1)  $\{R \rightarrow D\}$  link: Towards ensuring low delay, the  $\{R \rightarrow D\}$  links are prioritized whenever the UAV buffers are not empty. The buffer space is equally allocated to each maritime node, thus being divided in  $N$  sub-buffers, from which, the selected UAV forwards to the shore BS  $n$  packets, where  $n \leq N$ . Adopting such an algorithm, where buffer status is considered in the selection, allows the selected UAV to avoid overflowing the sub-buffer space of one or more sources, thus preserving the diversity of the MCN. In addition, in the  $\{R \rightarrow D\}$  link, CSIT is assumed to be available, as it is required at each UAV to determine the amount of data that can be successfully transmitted to the shore BS. So, although a UAV might fulfill the buffer status criterion of mIoT – NOMA, its  $\{R \rightarrow D\}$  link might not be able to support the data rate for successful delivery of the combined packet to the shore BS.

2)  $\{S \rightarrow R\}$  link: In cases where all the  $\{R \rightarrow D\}$  links are in outage, due to fading or empty UAV buffers, mIoT – NOMA employs simultaneous  $\{S \rightarrow R\}$  transmissions by the  $N$  maritime nodes. Thus, instead of relying on fixed user ordering, the UAVs consider CSI at the reception to determine the decoding order, thus maximizing the probability for successful SIC. More specifically, mIoT – NOMA uses the UAV buffers to store packets, even when SIC is not able to decode the packets of all  $N$  maritime nodes. The UAVs

store the successfully decoded packets from different sources, considering that the respective sub-buffers are not full. As mIoT – NOMA allows packets from a subset of the maritime nodes to be stored and transmitted, it is possible that the number of packets, residing in each sub-buffer will differ.

3) mIoT – NOMA operation: In general, efficient NOMA relies on pairing together highly asymmetric users, in the sense of either channel conditions, rate requirements or both. Thus, in our maritime topology, the availability of multiple buffer-assisted UAVs, provides increased degrees of freedom for mIoT – NOMA to avoid outages in the MCN. Moreover, UAV selection through mIoT – NOMA can leverage these DoF with low complexity, employing broadcasting by the sources without power control or highly complex pairing algorithms, avoiding CSIT in the  $\{S \rightarrow R\}$  links, relying instead on buffer status information and CSIT at the UAVs to operate. More specifically, in the  $\{S \rightarrow R\}$  links, dynamic user ordering at the relays requires only local CSI, in order to form the set  $\mathcal{F}_{SR}^n$ , while CSIT is used in the  $\{R \rightarrow D\}$  links to determine the links belonging in set  $\mathcal{F}_{RD}^n$ . Also, as a multi-UAV MCN is considered, power control of the transmit power employed by the maritime sources to enhance channel asymmetries might not be practical, as improving the chances of SIC at one UAV can degrade the performance of SIC at another UAV. So, in mIoT – NOMA, each maritime source transmits with fixed and equal power levels. Algorithm 1 describes the operation of mIoT – NOMA at an arbitrary time-slot.

---

#### Algorithm 1 mIoT – NOMA UAV selection

---

```

1: input  $\mathcal{F}_{RD}^n, n \in \{1, 2, \dots, N\}$ 
2: if  $\mathcal{F}_{RD}^n = \emptyset, \forall n$  then
3:   The  $N$  sources broadcast their packets to the  $K$  UAVs.
4:    $Q_j \leftarrow Q_j + r_j^\dagger, r_j^\dagger \in \{r_{\min}, \dots, r_{\max}\} \quad \forall j \in \mathcal{F}_{SR}^m, m \in \{1, 2, \dots, N\}$ 
5: else
6:    $n' = \arg \max_n \mathcal{F}_{RD}^n$ 
7:    $i' = \arg \max_{i \in \mathcal{F}_{RD}^{n'}} Q_{i, S_i}$ 
8:   if more than one UAVs have the same maximum sub-buffer length then
9:      $i^*$  is chosen randomly from the set of UAVs in  $i'$ .
10:  else
11:     $i^* = i'$ 
12:  end if
13:   $Q_i^* \leftarrow Q_i^* - r_i^*, r_i^* \in \{r_{\min}, \dots, r_{\max}\}$ 
14: end if
15: Output Link  $\{R_{i^*} \rightarrow D\}$  is activated to transmit with rate  $r_i^* \in \{r_{\min}, \dots, r_{\max}\}$  to the shore BS or the set of links in  $\mathcal{F}_{SR}^n$  receive packets of size  $r^\dagger \in \{r_{\min}, \dots, r_{\max}\}$  from  $n$  nodes via NOMA broadcasting, where  $n \leq N$ .

```

---

### IV. PERFORMANCE EVALUATION

Here, average sum-rate results for mIoT – NOMA and OMA are presented. A network with three maritime sources is considered, comprising a USV transmitting with rate  $r_{\text{USV}} \in \{4, 5\}$  bps/Hz and two buoys, each transmitting with rate

TABLE I  
SIMULATION PARAMETERS

Parameter	Value
No. of UAVs $K$	{2, 4, 6}
No. of transmissions per transmit power value	$10^4$
Buffer size $L$	100 bits
Transmission rate $r_{USV}$	{4, 5} bps/Hz
Transmission rate $r_{Buoy}$	0.5 bps/Hz
Transmit power range of each transmitter $P_{T,max}$	[0, 30] dBm
Noise power at each receiver $\sigma^2$	-107 dBm
Carrier frequency $f$	2 GHz
Propagation constants $\alpha, b, \eta_{LoS}, \eta_{NLoS}$	5.0188, 0.3511, 0.1, 21
UAV altitude $h_U$	300 m

$r_{Buoy} = 0.5$  bps/Hz. An equivalent OMA algorithm is included in the comparisons where at each time-slot, a specific maritime source is transmitting, either in the  $\{S \rightarrow R\}$  or in the  $\{R \rightarrow D\}$  links. For fairness, the required rate for successful transmission by each source is set to three times the target rate, since in NOMA, all sources concurrently transmit at each time-slot. Regarding the coordinates of the shore BS, it is assumed to be located at (0, 0, 10) m while the UAVs and maritime sources are assumed to be randomly deployed in a maritime area with x-axis coordinates taking values from [0, 100] m and y-axis coordinates taking values from [-100, 100] m, remaining fixed throughout the transmission's duration, with the UAVs flying at a height of 300 m. Finally, in order to provide further insights on the performance of mIoT – NOMA, various cases of  $K$ , and  $r_{USV}$  are evaluated. The simulation parameters adopt the values in [11] and are listed in Table I.

Fig. 2 depicts the average sum-rate results for varying  $K$  when  $r_{USV} = 4$  bps/Hz and  $r_{Buoy} = 0.5$  bps/Hz. For mIoT – NOMA, as the number of UAVs increases, performance is significantly improved. More specifically, when additional UAVs are added to the MCN, higher probability for asymmetric channel qualities among the maritime sources is observed. So, combined with the existing rate asymmetry, the dynamic decoding ordering allows more efficient SIC processing at the UAVs. On the contrary, OMA struggles to satisfy the USV rate requirement for low  $P_T$  values and experiences significant sum-rate losses until 20 dbm. For higher  $P_T$  values, mIoT – NOMA performance saturates, as SIC cannot provide further performance gains while OMA exploits the high SNR regime to satisfy all rate requirements and offers improved performance due to interference-free reception.

The second sum-rate comparison is shown in Fig. 3 where a higher  $r_{USV} = 5$  bps/Hz is considered. Here, the superiority of mIoT – NOMA is clear for a much wider SNR range, although a performance ceiling is seen after 20 dbm. Again, increasing  $K$  facilitates NOMA operation due to higher link diversity and asymmetry. As for OMA, it provides higher sum-rate after 28 dbm for  $K = 2, 4$  but completely fails to satisfy  $r_{USV}$  until 16 dbm. When  $K = 6$ , OMA reaches the performance of mIoT – NOMA only at 30 dbm.

From the two comparisons, it is evident that mIoT – NOMA can better support MCNs for a broad range of SNR while OMA is better suited in cases where

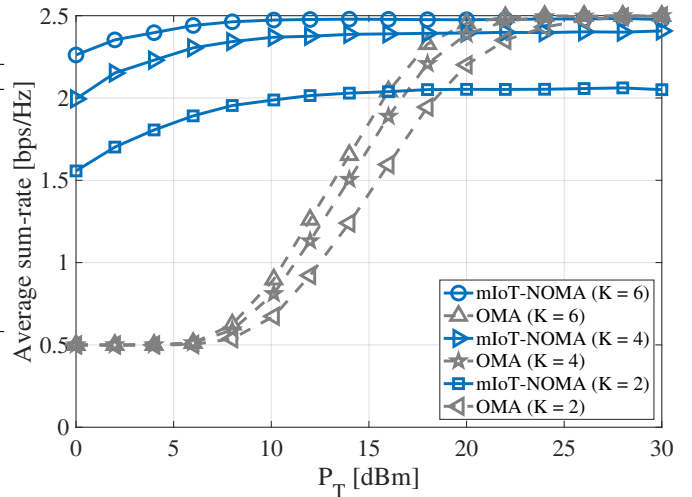


Fig. 2. Average sum-rate comparisons for different multiple access algorithms and number of UAVs when  $r_{USV} = 4$  bps/Hz and  $r_{Buoy} = 0.5$  bps/Hz.

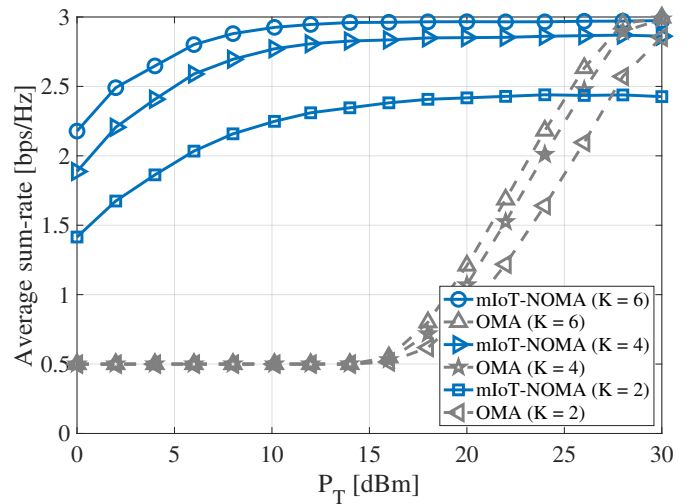


Fig. 3. Average sum-rate comparisons for different multiple access algorithms and number of UAVs when  $r_{USV} = 5$  bps/Hz and  $r_{Buoy} = 0.5$  bps/Hz.

higher  $P_T$  is used in services with high rate requirements. Thus, an optimal solution would entail a hybrid algorithm, switching among NOMA and OMA in order to exploit both SIC and interference-free reception when SIC fails.

## V. CONCLUSIONS AND FUTURE DIRECTIONS

In this paper, a maritime Internet-of-Things (IoT) topology was studied, where multiple nodes, such as unmanned surface vehicles (USVs) and buoys aim to transmit their data towards a shore base station (BS). However, due to excessive fading, direct connectivity is not feasible and multiple buffer-aided unmanned aerial vehicles (UAVs) are deployed to act as relays. In this context, we adopt non-orthogonal multiple access (NOMA) with dynamic decoding ordering at the UAVs to simultaneously receive multiple signals from the maritime nodes. The proposed algorithm, namely mIoT – NOMA exploits these techniques and the flexibility of data caching to

maximize the network sum-rate, adhering to the service requirements of the maritime nodes. Simulation results highlight the gains of mIoT – NOMA over orthogonal multiple access alternatives, in terms of average sum-rate for different multi-UAV maritime topologies and USV rate requirements.

Ongoing research is focusing on the following areas:

- Comparisons highlighted that NOMA and OMA provide better performance for different SNR regimes. Thus, a hybrid NOMA/OMA algorithm should be developed to exploit the advantages of both multiple access techniques.
- The synergy among shore/aerial/surface/underwater nodes entails high coordination overheads, especially in centralized deployments. Thus, distributed approaches, exploiting machine learning to derive channel statistics, beamforming vectors and mobility patterns can be integrated in mIoT – NOMA [27], [28].
- Another domain that must be explored is the integration of open and programmable communications solutions, such as Open Radio Access Network (O-RAN) and network function virtualization (NFV) to enhance the scalability and service optimization in cases with massive numbers of maritime nodes [29], [30].

#### ACKNOWLEDGMENTS

This work was supported in part by the ICOS (Towards a functional continuum operating system) Project funded from the European Union’s HORIZON research and innovation programme under grant agreement No 101070177 (<https://www.icos-project.eu/>).

#### REFERENCES

- [1] N. Nomikos, E. T. Michailidis, P. Trakadas, D. Vouyioukas, H. Karl, J. Martrat, T. Zahariadis, K. Papadopoulos, and S. Voliotis, “A UAV-based moving 5G RAN for massive connectivity of mobile users and IoT devices,” *Vehicular Communications*, vol. 25, p. 100250, 2020.
- [2] P. Trakadas, N. Nomikos, E. T. Michailidis, T. Zahariadis, F. M. Facca, D. Breitgand, S. Rizou, X. Masip, and P. Gkonis, “Hybrid clouds for data-intensive, 5g-enabled iot applications: An overview, key issues and relevant architecture,” *Sensors*, vol. 19, no. 16, p. 3591, Aug 2019.
- [3] M. Vaezi, A. Azari, S. R. Khosravirad, M. Shirvanimoghaddam, M. M. Azari, D. Chasaki, and P. Popovski, “Cellular, wide-area, and non-terrestrial IoT: A survey on 5G advances and the road toward 6G,” *IEEE Communications Surveys & Tutorials*, vol. 24, no. 2, pp. 1117–1174, 2022.
- [4] T. Xia, M. M. Wang, J. Zhang, and L. Wang, “Maritime internet of things: Challenges and solutions,” *IEEE Wireless Communications*, vol. 27, no. 2, pp. 188–196, 2020.
- [5] M. M. Wang, J. Zhang, and X. You, “Machine-type communication for maritime internet of things: A design,” *IEEE Communications Surveys & Tutorials*, vol. 22, no. 4, pp. 2550–2585, 2020.
- [6] Y. Wang, W. Feng, J. Wang, and T. Q. S. Quek, “Hybrid satellite-UAV-terrestrial networks for 6G ubiquitous coverage: A maritime communications perspective,” *IEEE Journal on Selected Areas in Communications*, vol. 39, no. 11, pp. 3475–3490, 2021.
- [7] P. S. Bithas, E. T. Michailidis, N. Nomikos, D. Vouyioukas, and A. G. Kanatas, “A survey on machine-learning techniques for UAV-based communications,” *Sensors*, vol. 19, no. 23, 2019.
- [8] N. Nomikos, P. K. Gkonis, P. S. Bithas, and P. Trakadas, “A survey on uav-aided maritime communications: Deployment considerations, applications, and future challenges,” *IEEE Open Journal of the Communications Society*, pp. 1–1, 2022.
- [9] N. Nomikos, P. Trakadas, A. Hatziefremidis, and Voliotis, “Full-duplex noma transmission with single-antenna buffer-aided relays,” *Electronics*, vol. 8, no. 12, p. 1482, Dec 2019. [Online]. Available: <http://dx.doi.org/10.3390/electronics8121482>
- [10] N. Nomikos, E. T. Michailidis, P. Trakadas, D. Vouyioukas, T. Zahariadis, and I. Krikidis, “Flex-NOMA: Exploiting buffer-aided relay selection for massive connectivity in the 5G uplink,” *IEEE Access*, vol. 7, pp. 88 743–88 755, 2019.
- [11] R. Tang, W. Feng, Y. Chen, and N. Ge, “NOMA-based UAV communications for maritime coverage enhancement,” *China Communications*, vol. 18, no. 4, pp. 230–243, 2021.
- [12] S. Guan, J. Wang, C. Jiang, R. Duan, Y. Ren, and T. Q. S. Quek, “MagicNet: The maritime giant cellular network,” *IEEE Communications Magazine*, vol. 59, no. 3, pp. 117–123, 2021.
- [13] F. S. Alqurashi, A. Trichili, N. Saeed, B. S. Ooi, and M.-S. Alouini, “Maritime communications: A survey on enabling technologies, opportunities, and challenges,” *IEEE Internet of Things Journal*, pp. 1–1, 2022.
- [14] “Starlink Maritime,” <https://www.starlink.com/maritime>, 2008, [Online; accessed September, 2022].
- [15] Y. Huo, X. Dong, and S. Beatty, “Cellular communications in ocean waves for maritime internet of things,” *IEEE Internet of Things Journal*, vol. 7, no. 10, pp. 9965–9979, 2020.
- [16] P. S. Bithas, V. Nikolaidis, A. G. Kanatas, and G. K. Karagiannidis, “UAV-to-ground communications: Channel modeling and UAV selection,” *IEEE Transactions on Communications*, vol. 68, no. 8, pp. 5135–5144, 2020.
- [17] X. Li, W. Feng, J. Wang, Y. Chen, N. Ge, and C.-X. Wang, “Enabling 5G on the ocean: A hybrid satellite-UAV-terrestrial network solution,” *IEEE Wireless Communications*, vol. 27, no. 6, pp. 116–121, 2020.
- [18] J. Wang, H. Zhou, Y. Li, Q. Sun, Y. Wu, S. Jin, T. Q. S. Quek, and C. Xu, “Wireless channel models for maritime communications,” *IEEE Access*, vol. 6, pp. 68 070–68 088, 2018.
- [19] A. Zolich, D. Palma, K. Kansanen, K. Fjørtoft, J. Sousa, K. H. Johansson, Y. Jiang, H. Dong, and T. A. Johansen, “Survey on communication and networks for autonomous marine systems,” *Journal of Intelligent & Robotic Systems*, vol. 95, pp. 789–813, 2022.
- [20] H. Luo, J. Wang, F. Bu, R. Ruby, K. Wu, and Z. Guo, “Recent progress of air/water cross-boundary communications for underwater sensor networks: A review,” *IEEE Sensors Journal*, vol. 22, no. 9, pp. 8360–8382, 2022.
- [21] X. Fang, W. Feng, Y. Wang, Y. Chen, N. Ge, Z. Ding, and H. Zhu, “NOMA-based hybrid satellite-UAV-terrestrial networks for 6G maritime coverage,” *IEEE Transactions on Wireless Communications*, pp. 1–1, 2022.
- [22] R. Ma, R. Wang, G. Liu, H.-H. Chen, and Z. Qin, “UAV-assisted data collection for ocean monitoring networks,” *IEEE Network*, vol. 34, no. 6, pp. 250–258, 2020.
- [23] R. Ma, R. Wang, G. Liu, W. Meng, and X. Liu, “UAV-aided cooperative data collection scheme for ocean monitoring networks,” *IEEE Internet of Things Journal*, vol. 8, no. 17, pp. 13 222–13 236, 2021.
- [24] A. A. Nasir, H. D. Tuan, T. Q. Duong, and H. V. Poor, “Uav-enabled communication using noma,” *IEEE Transactions on Communications*, vol. 67, no. 7, pp. 5126–5138, 2019.
- [25] Y. Chen, W. Feng, and G. Zheng, “Optimum placement of uav as relays,” *IEEE Communications Letters*, vol. 22, no. 2, pp. 248–251, 2018.
- [26] J. Wang, B. Xia, K. Xiao, Y. Gao, and S. Ma, “Outage performance analysis for wireless non-orthogonal multiple access systems,” *IEEE Access*, vol. 6, pp. 3611–3618, 2018.
- [27] N. Nomikos, M. S. Talebi, T. Charalambous, and R. Wichman, “Bandit-based power control in full-duplex cooperative relay networks with strict-sense stationary and non-stationary wireless communication channels,” *IEEE Open Journal of the Communications Society*, vol. 3, pp. 366–378, 2022.
- [28] S. Lavdas, P. K. Gkonis, Z. Zinonos, P. Trakadas, L. Sarakis, and K. Papadopoulos, “A machine learning adaptive beamforming framework for 5g millimeter wave massive mimo multicellular networks,” *IEEE Access*, vol. 10, pp. 91 597–91 609, 2022.
- [29] A. Giannopoulos, S. Spantideas, N. Kapsalis, P. Gkonis, L. Sarakis, C. Capsalis, M. Vecchio, and P. Trakadas, “Supporting intelligence in disaggregated open radio access networks: Architectural principles, ai/ml workflow, and use cases,” *IEEE Access*, vol. 10, pp. 39 580–39 595, 2022.
- [30] P. A. Karkazis, K. Railis, S. Prekas, P. Trakadas, and H. C. Leligou, “Intelligent network service optimization in the context of 5g/nfv,” *Signals*, vol. 3, no. 3, pp. 587–610, Sep 2022.